

REVIEW

Radiological Vascular Anatomy of the Caudate Lobe of the Liver Required for Transarterial Chemoembolization of Hepatocellular Carcinoma

Shiro Miyayama

Department of Diagnostic Radiology, Fukui-ken Saiseikai Hospital, Japan

Abstract:

The caudate lobe is located between the bilateral hepatic lobes and is divided into three subsegments: the Spiegel lobe, paracaval portion, and caudate process. The caudate artery arises from various sites of the bilateral hepatic arteries as an independent branch, common trunk, or arcade. Extrahepatic arteries can enter the caudate lobe mainly by the right inferior phrenic artery. The caudate artery also supplies the main bile duct and posterior aspect of segment IV. Although catheterization into the caudate artery is occasionally difficult because of its small size and sharp angulation, selective embolization of a tumor feeder is a significant prognostic factor in patients with hepatocellular carcinoma originating there. Therefore, we should recognize the peculiarity of its vascular anatomy and should be familiar with catheterization and embolization techniques.

Keywords:

caudate lobe of the liver, vascular anatomy, hepatocellular carcinoma, transarterial chemoembolization

Interventional Radiology 2023; 8(3): 118-129
<https://doi.org/10.22575/interventionalradiology.2022-0046>
<https://ir-journal.jp/>

Introduction

The caudate lobe is located between the bilateral hepatic lobes, near the hepatic hilar plate and inferior vena cava (IVC). It is also adjacent to the bare area of the liver. Because of this anatomical location, hepatocellular carcinoma (HCC) arising there is difficult to treat. Surgical resection is a curative option, but it is associated with a high mortality rate and a high recurrence rate [1, 2]. Percutaneous ablation therapy, such as ethanol injection and microwave or radiofrequency ablation, is a challenging option [3-5], and it might also be technically difficult because of a deep tumor location and adjacent large vessels. Therefore, transarterial chemoembolization (TACE) plays an important role in the treatment of HCC originating in the caudate lobe, although it is also difficult because of the complex arterial blood supply and frequent unsuccessful catheterization into a tumor feeder [6].

The advancement of TACE techniques has improved the local control effect of TACE on unresectable HCC [7-12], but the caudate lobe is still a difficult location to complete effective TACE. Thus, the purpose of this paper is to describe the radiological vascular anatomy required to perform

effective TACE for HCC in the caudate lobe.

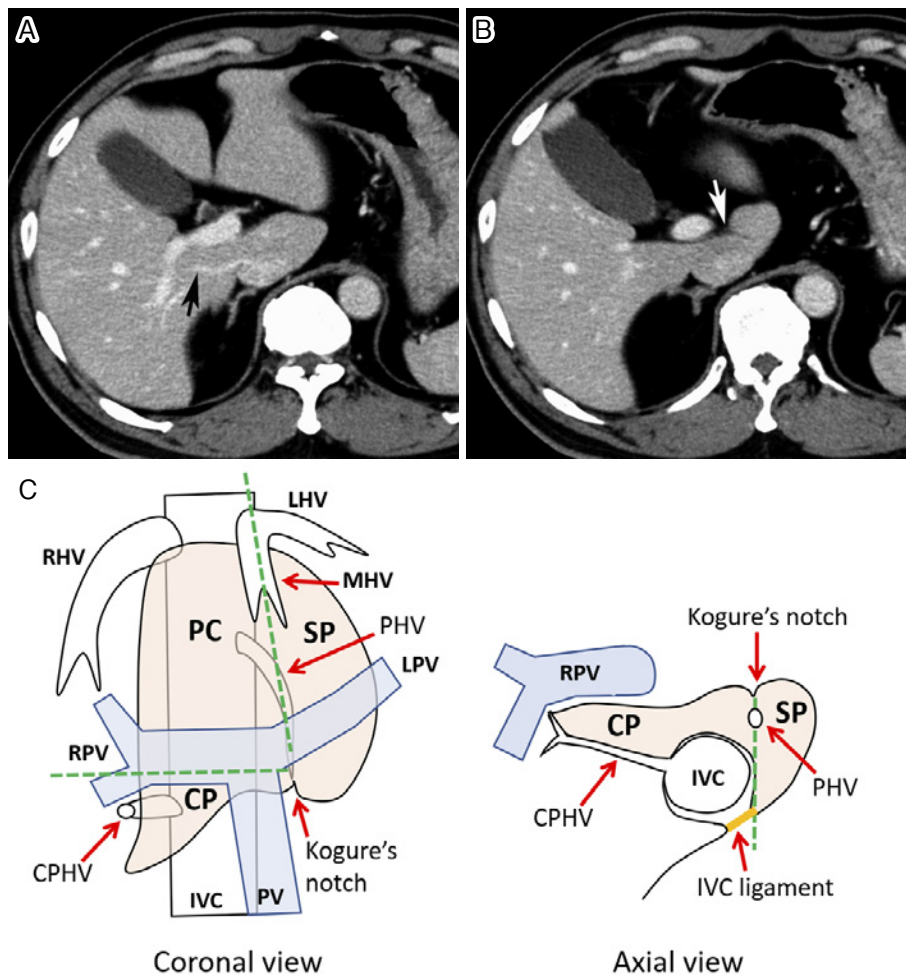
Caudate Lobe Anatomy

According to Kumon's classification, the caudate lobe is divided into three subsegments on the basis of the portal vein ramification: the Spiegel lobe (SP), paracaval portion (PC), and caudate process (CP). SP is a protuberant hepatic portion to the left of the intrahepatic IVC. PC is in front of the intrahepatic IVC and is surrounded by the right and middle hepatic veins. PC also reaches the liver surface beneath the diaphragm in most livers [13]. Anatomically, the external notch of the caudate lobe (Kogure's notch), corresponding to the route of the proper hepatic vein, divides SP and PC (**Fig. 1**) [14], but it occasionally cannot be demonstrated on CT and MRI. CP is a tongue-like projection between the IVC and right portal vein, below PC. PC and CP are divided by the height of the right portal pedicle [13]. The anatomical landmark between CP and segment VI is the caudate processus hepatic vein (**Fig. 1**) [15], but it is also occasionally difficult to identify on imaging. Moreover, there are no landmarks between PC and segment VIII. Therefore, the border of the caudate lobe is unclear in parts,

Corresponding author: Shiro Miyayama, s-miyayama@fukui.saiseikai.or.jp

Received: January 16, 2023, Accepted: March 23, 2023

Copyright © The Japanese Society of Interventional Radiology



Abbreviations: CP, caudate process; CPHV, caudate processus hepatic vein; IVC, inferior vena cava; LHV, left hepatic vein; LPV, left portal vein; MHV, middle hepatic vein; PC, paracaval portion; PHV, proper hepatic vein; PV, portal vein; RHV, right hepatic vein; RPV, right portal vein; SP, Spiegel lobe

Figure 1. Anatomical landmarks of the caudate lobe. A. The caudate processus hepatic vein (arrow). B. The external notch of the caudate lobe (Kogure's notch) (arrow). C. Schematic drawing of the anatomical landmarks of the three subsegments of the caudate lobe.

and the size of the caudate lobe varies individually.

Caudate Artery Anatomy

The caudate lobe is supplied by 3-6 portal branches [13]. Therefore, it is considered that the same number of caudate arteries accompanying the portal veins may enter the caudate lobe. However, identifying the caudate artery on arteriograms is frequently difficult because it is usually small and overlaps other hepatic arterial branches [6].

The advancement of imaging modalities and catheter-guidewire technologies has made it possible to visualize the caudate artery more clearly. In a report by Oshiro et al. [16], CT during hepatic arteriography (CTHA) demonstrated 1.1 ± 0.8 (range, 0-3) caudate arteries arising from the right hepatic artery (RHA) and 1.5 ± 0.7 (range, 1-4) ones arising from the left hepatic artery (LHA). They divided the caudate artery into two branches: the right caudate branch

supplying CP and PC, and the left caudate branch supplying SP. The branching pattern of the caudate artery was also divided into three types: an independent branch (type 1), a common trunk of the right and left caudate branches (type 2), and a branch arising from the communicating artery (type 3). The incidences were 30% for type 1, 12% for type 2, 34% for type 3, 8% for type 1 plus type 2, and 16% for type 1 plus type 3. Forty-seven (22 right and 25 left branches) independent branches (type 1) were identified in 27 of 50 patients, and the right branch arose from the posterior segmental artery of RHA (50%), RHA (32%), anterior segmental artery of RHA (14%), and middle hepatic artery (MHA) (4%). By contrast, the left branch arose from LHA (52%), posterior segmental artery of RHA (20%), MHA (16%), and RHA (12%). A common trunk formed by the right and left branches (type 2) was seen in 10 of 50 patients, and it arose from LHA (40%), posterior segmental artery of RHA (20%), RHA (20%), anterior segmental artery

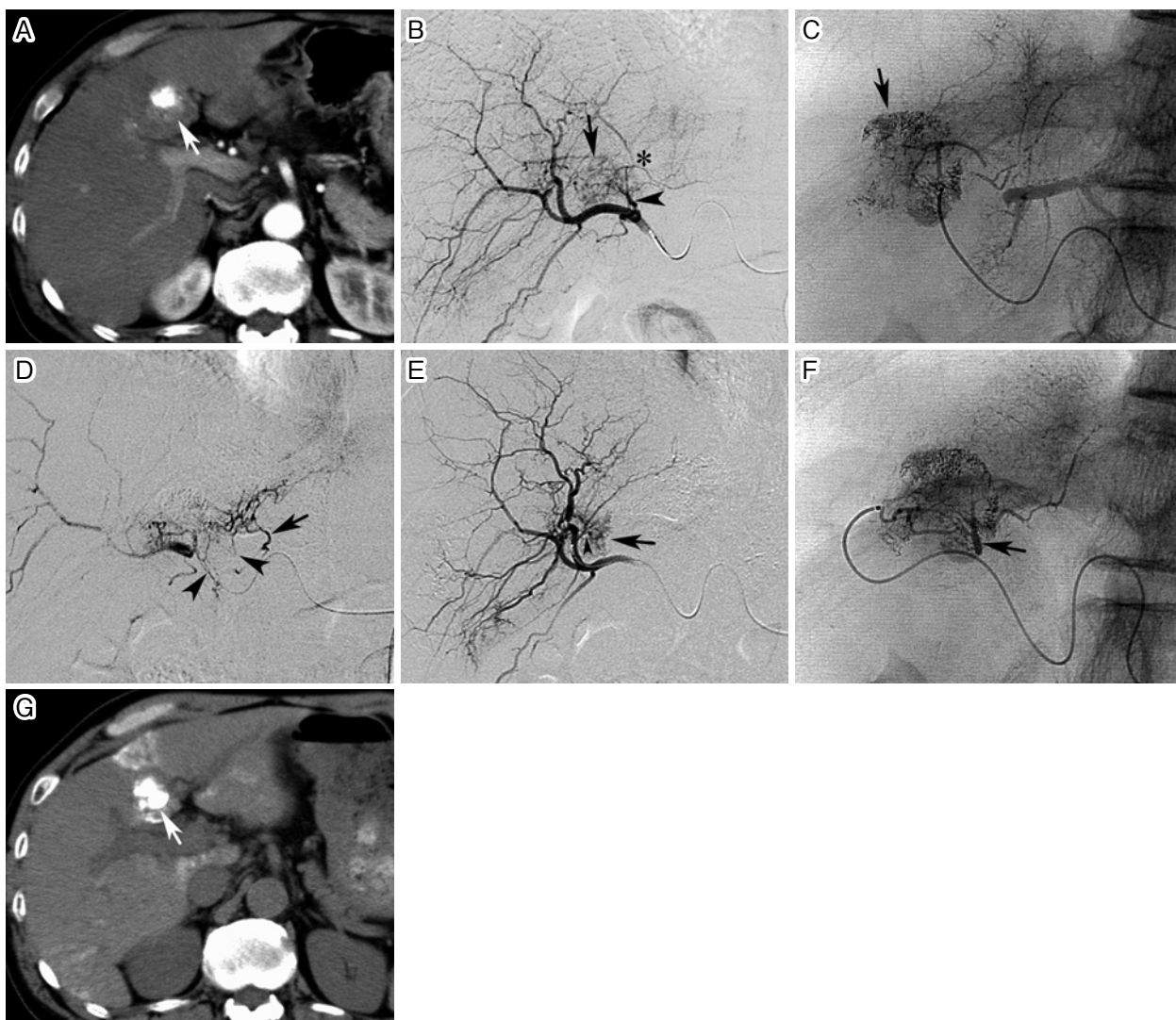


Figure 2. Blood supply to the posterior aspect of segment IV (PASIV) from the caudate artery.

A. Arterial-phase CT shows a recurrent hepatocellular carcinoma in PASIV (arrow). B. Right hepatic arteriogram demonstrates a tumor stain (arrow). The arrowhead indicates the middle hepatic artery, and the asterisk indicates the caudate artery (the Spiegel lobe branch). C. First, the caudate artery was embolized, and iodized oil was accumulated in the tumor (arrow). D. Selective arteriogram of this branch performed immediately after transarterial chemoembolization (TACE) demonstrates the caudate artery arising from the left hepatic artery (LHA) (arrow) and arterial plexus around the bilateral hepatic ducts and common hepatic duct (arrowheads) through the anastomoses. E. Right hepatic arteriogram shows the residual tumor stain (arrow) supplied by another caudate artery (the paracaval branch) arising from the anterior segmental artery of the right hepatic artery (arrowhead). F. During TACE of this branch, the previously embolized caudate artery was opacified with iodized oil passing through the anastomoses (arrow). Thereafter, the medial subsegmental artery arising from LHA, which was a tumor feeder on the initial TACE, was embolized, although selective arteriogram of this branch did not show tumor stains (not shown). G. Unenhanced CT performed 1 week after TACE shows iodized oil accumulation in the tumor in PASIV (arrow). Figures 2A–D, F, and G reprinted from Ref. [36] with permission.

of RHA (10%), and MHA (10%). A communicating artery (type 3) was seen in 25 of 50 patients; between RHA and LHA (35%); between the posterior segmental artery of RHA, RHA, and LHA (12%); between the posterior segmental artery of RHA and LHA (12%); and others (42%).

From the right hepatic arterial system, the caudate artery can arise anywhere until the proximal portion of the anterior and posterior segmental arteries of RHA, and multiple caudate arteries arising from different origins are demonstrated in most cases (Fig. 2-5). The caudate artery also arises from

LHA until the umbilical portion and from the proximal portion of MHA or medial subsegmental artery of LHA (A4) (Fig. 2; Videos 1 and 2). Moreover, the caudate artery infrequently arises from the cystic artery with a common trunk and from the proper hepatic, common hepatic, or extrahepatic artery, such as the right gastric and inferior phrenic arteries (IPA) (Fig. 6) [17-20].

Among the caudate arteries arising from RHA, the PC branch runs upwardly whereas the SP branch runs to the left (Fig. 2 and 3). These branches frequently arise as a common

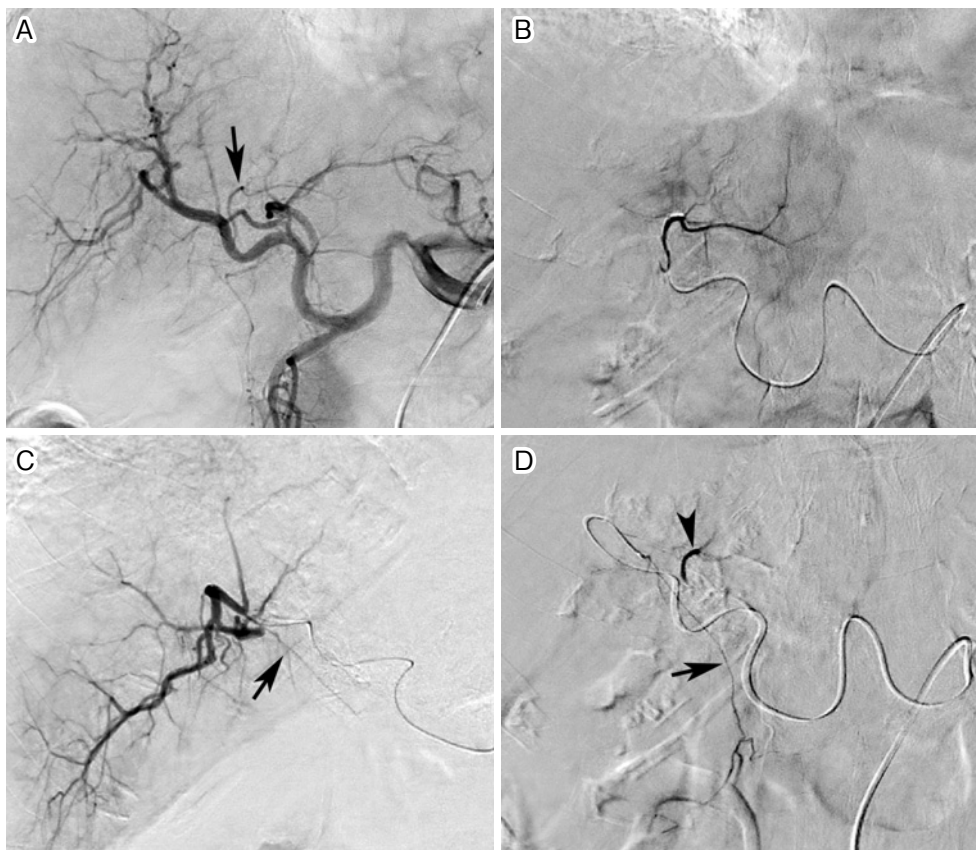


Figure 3. Communication between the caudate artery and the 9 o'clock artery.

A. Celiac arteriogram shows the Spiegel lobe (SP) branch of the caudate artery arising from the right hepatic artery (RHA) (arrow). B. Selective arteriogram of the SP branch. C. Selective arteriogram of the posterior segmental artery of RHA shows the caudate process branch of the caudate artery (arrow). D. Selective arteriogram of this branch demonstrates the previously embolized SP branch (arrowhead) and the 9 o'clock artery through the anastomoses (arrow).

trunk (**Fig. 4**). A typical hepatogram indicating the contour of SP is demonstrated by the selective arteriogram of the SP branch (**Fig. 6**). The PC branch also arises from the proximal portion of the anterior segmental artery of RHA and runs to the upper left. The CP branch usually mimics a branch of the posterior segmental artery of RHA (**Fig. 3**). Among the caudate arteries arising from LHA, the SP branch usually mimics the lateral segmental artery of LHA and the PC branch mimics A4 [18, 20]. The caudate arteries are usually connected with each other and with MHA or A4 (**Fig. 2-6**) [16, 21, 22].

Blood Supply to the Caudate Lobe from the Extrahepatic Artery

It is well known that the right IPA occasionally supplies the tumor in the caudate lobe [17-20, 23-27]. The first branch of the right IPA, called the suprarenal branch, mainly supplies the dorsal part of SP, together with branches arising from the main trunk or from the proximal portion of the anterior (ascending) and posterior (descending) branches [24, 25]. These branches penetrate the IVC ligament and run around the IVC, and finally reach the caudate lobe (**Fig. 7**) [24]. The right IPA can also supply the dorsal part of PC

and CP when the arterial circulation of the caudate lobe is attenuated by previous TACE [24]. The right IPA is the main extrahepatic blood source of HCC in the caudate lobe, especially a recurrent tumor after TACE, as Woo et al. [26] reported that it supplied 88.6% of tumors in the caudate lobe that were fed by extrahepatic arteries. The left or right gastric, dorsal pancreatic, right adrenal, right renal capsular, and 3 and 9 o'clock arteries are also possible collateral vessels to HCC in the caudate lobe, especially when the caudate artery and right IPA were previously embolized [18, 26]. Additionally, the right IPA infrequently supplies the caudate lobe on the initial TACE [24].

Blood Supply to the Bile Duct from the Caudate Artery

Anatomically, extra- and intrahepatic bile ducts are surrounded by a vascular plexus that is composed of branches arising directly from RHA, LHA, and their segmental branches, and indirectly from the gastroduodenal artery through the 3 and 9 o'clock arteries [28, 29]. The plexus around the right and left hepatic ducts is continuous with a plexus surrounding the common hepatic duct and common bile duct. The caudate artery gives several branches to the

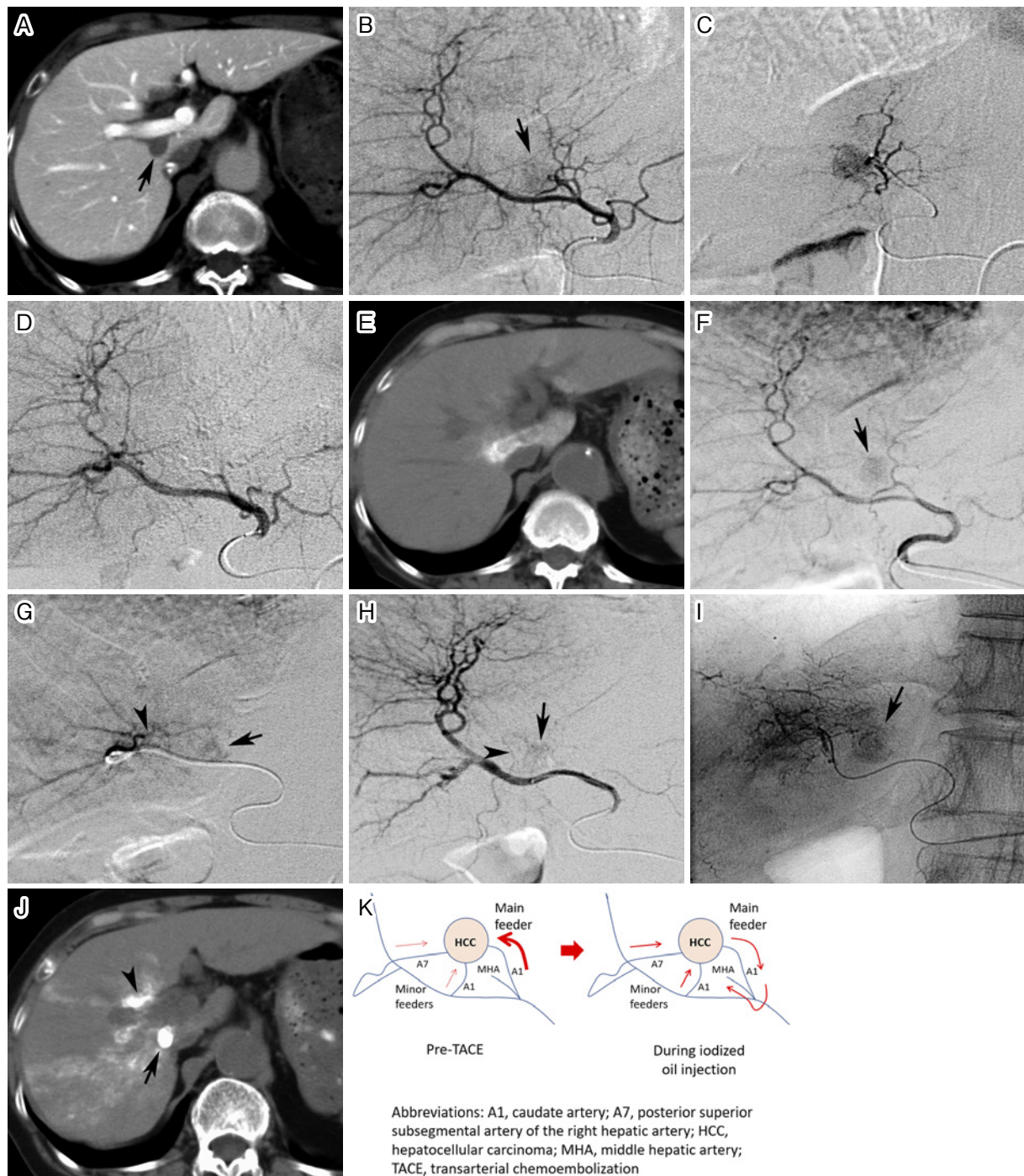


Figure 4. Unsuccessful transarterial chemoembolization (TACE) of hepatocellular carcinoma (HCC) in the caudate lobe.

A. CTAP shows a small HCC in the paracaval portion (PC) of the caudate lobe (arrow). B. Proper hepatic arteriogram shows a tumor stain (arrow). C. Selective arteriogram of the caudate artery (a common truck of the Spiegel lobe [SP] and PC branches) demonstrates a tumor stain. Thus, TACE was performed at this point. D. Proper hepatic arteriogram performed immediately after TACE shows the disappearance of the tumor stain. Additionally, the middle hepatic artery is inadvertently embolized by overflowed embolic agents. E. However, iodized oil is not accumulated in the tumor on unenhanced CT performed 1 week after TACE, although iodized oil is injected into the entire SP and PC. F. The tumor was viable and additional TACE was performed 6 months later. Proper hepatic arteriogram shows a tumor stain (arrow), although the previously embolized caudate artery is occluded. G. The tumor (arrow) is partially supplied by the posterior superior subsegmental artery of the right hepatic artery (RHA) (A7) (arrowhead). Thus, A7 was embolized first. H. Right hepatic arteriogram performed after TACE of A7 shows the residual tumor (arrow) supplied by the caudate artery arising from RHA (arrowhead). I. Thereafter, the branch was selectively embolized. The arrow indicates the tumor. J. Unenhanced CT performed 1 week after additional TACE shows dense iodized oil accumulation in the tumor (arrow). Iodized oil is also accumulated in the posterior aspect of segment IV (arrowhead). K. Schematic presentation of a possible cause of unsuccessful TACE due to changes in the hemodynamics of a tumor during the first TACE procedure.

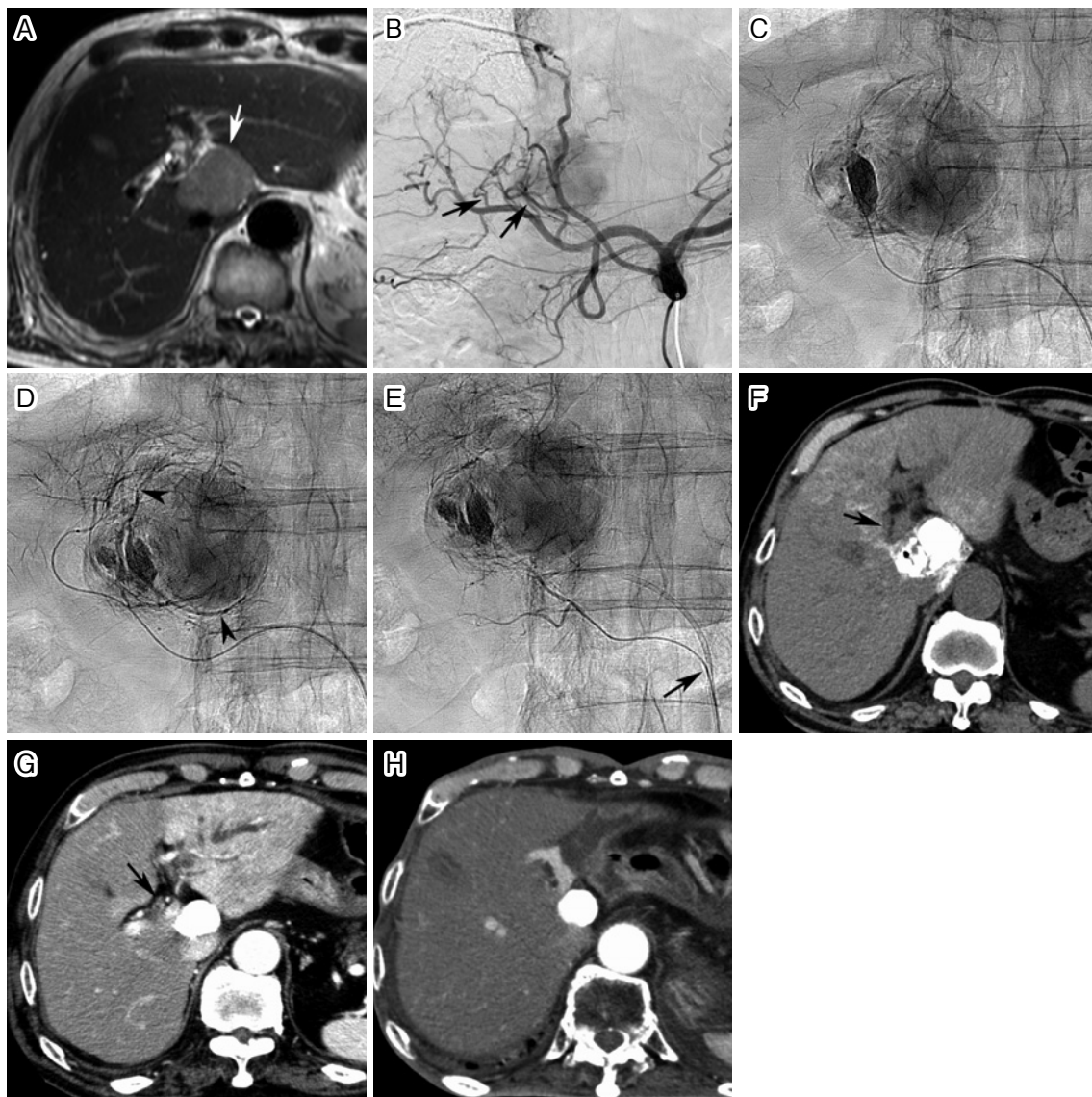


Figure 5. Bile duct stricture following transarterial chemoembolization (TACE) of the caudate artery. A. T2-weighted MRI depicts a tumor in the Spiegel lobe and paracaval portion of the caudate lobe (arrow). B. Celiac arteriogram shows a tumor stain supplied by two caudate arteries (arrows). C. First, TACE of the proximal caudate artery was performed. D. Thereafter, the distal caudate artery was embolized. During TACE of this branch, the proximal caudate artery that had been embolized first was retrogradely opacified (arrowheads). E. Finally, the first branch of the right inferior phrenic artery was selected through a large side hole (arrow) created on a 4-Fr twist catheter, and this branch was embolized, although selective arteriogram showed no obvious tumor stains. F. CT performed 1 week after TACE shows dense iodized oil accumulation in the tumor. Additionally, iodized oil faintly accumulates in the left hepatic duct (arrow). G. Arterial-phase CT performed 1 year after TACE shows the dilatation of the bile duct and segmental staining in the lateral segment of the left hepatic lobe due to the stricture of the left hepatic duct (arrow). H. Arterial-phase CT performed 7 years and 3 months after TACE shows marked bile duct dilatation and atrophy of the lateral segment of the left hepatic lobe, although the tumor has been well controlled.

hepatic duct plexus (**Fig. 2**) [16, 28], and A4 is also the main blood source of the left hepatic duct [30].

The most common vascular distribution of the biliary tract forms the arteries at 3 and 9 o'clock. There are also several anastomoses between the vascularization of the bile duct and other arteries, including the cystic, caudate, RHA, MHA or A4, and branches of the gastroduodenal artery (**Fig. 3**) [31]. The communicating arcade between the bilateral hepatic lobes is also present [16, 32], and it mainly connects be-

tween the caudate arteries or between the caudate artery and MHA or A4 (**Fig. 6**) [21]. The communicating arcade also forks into a few branches to the caudate lobe [16, 32].

A branch supplying the bile duct or connecting with the 3 and 9 o'clock arteries usually arises from the first and/or second branch of the caudate artery and MHA or A4 [22]. Therefore, it is very important to deeply advance a microcatheter into these arteries beyond the proximal branches when selective TACE is performed. Bile duct necrosis and

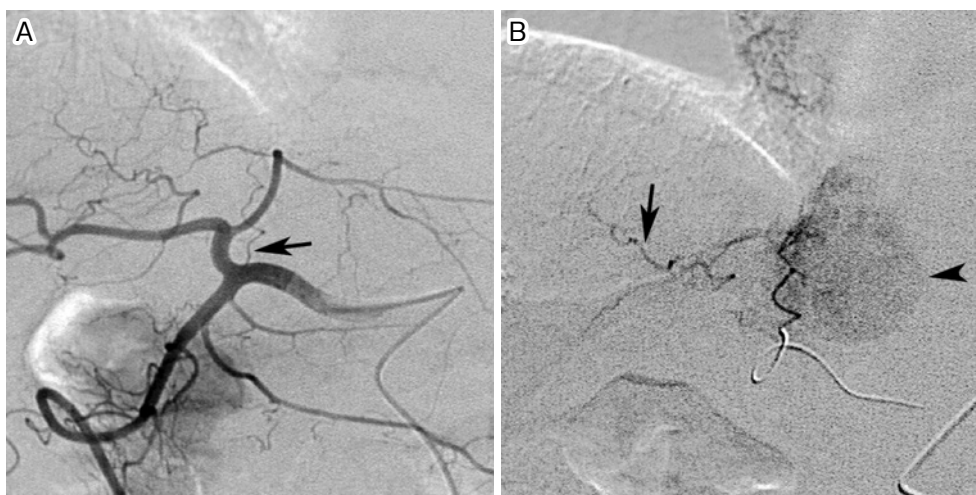


Figure 6. The caudate artery arising from the right gastric artery.

A. Common hepatic arteriogram shows the caudate artery arising from the right gastric artery (arrow). B. Selective arteriogram of the caudate artery demonstrates the communicating arcade between the caudate artery and the middle hepatic artery (arrow). A typical hepatogram of the Spiegel lobe is also seen (arrowhead).

stricture following TACE of the caudate artery typically develop at the common hepatic duct and/or right or left hepatic duct, corresponding to the blood supply from the caudate artery (**Fig. 5**) [21, 22].

Blood Supply to the Posterior Aspect of Segment IV from the Caudate Artery

Segment IV of the liver, at least the quadrate lobe, appears rather late during embryologic development, and this explains the marked variety in form and the numerous vascular and biliary variations [34]. It has been reported that some caudate portal branches may ascend posteriorly above the plane of the hepatic veins and supply the posterior aspect of segment IV (PASIV) [33]. In a report by Kobayashi et al. [34], PASIV was supplied by RHA in 8% of cases on CTHA. Conversely, CT performed 1 week after TACE of the caudate artery showed iodized oil accumulation in PASIV in 67% of cases, even if 87.9% of the embolized caudate arteries were arising from RHA (**Fig. 2 and 4**) [35]. This indicates that some injected iodized oil can enter the caudate lobe not only directly but also through the communicating arcade or microarterial communication in the hilar plate by superselective injection. By contrast, some tumors in the caudate lobe, especially recurrent tumors in PC after TACE, can also be supplied by A4 [36]. Therefore, there is another possibility that a small caudate branch may arise from MHA or A4 and that a small branch supplying PASIV may also arise from the caudate artery [37], although they are occasionally difficult to distinguish on arteriograms.

Variations of Tumor Feeders According to the Tumor Location in the Caudate Lobe

In our previous analysis of 88 caudate HCCs (36 in SP, 38 in PC, and 14 in CP) with a mean tumor diameter of

21.4 ± 11.0 mm (range, 8-62), 116 tumor feeders were identified. Among them, 27.6% of the tumor feeders arose from RHA; 20.7%, from LHA; 6%, from MHA or A4; 0.9%, from the proper hepatic artery; and 2.6%, from the extrahepatic artery [19]. However, these incidences might be easily changed by the number of tumors in each subsegment in the cohort. Additionally, the caudate arteries that did not supply the tumor were not counted, although they were identified by arteriogram. Therefore, the results do not cover the branching pattern of all caudate arteries, unlike the study using CTHA images [16].

The origins of the tumor-feeding caudate arteries differ among the three subsegment locations of HCC. HCCs located in SP were fed by the branches arising from the right and left hepatic arterial systems (the right-to-left ratio = 3:2). Additionally, extrahepatic vessels, such as the right IPA and right gastric artery, infrequently fed the tumors in the anterior or posterior part of SP. HCCs in PC were also fed by the branches arising from both hepatic arterial systems, with a lower frequency arising from the left hepatic arterial supply (the right-to-left ratio = 3:1). Conversely, HCCs in CP were dominantly fed by the branches arising from the right hepatic arterial system, mainly from the anterior or posterior segmental artery of RHA (the right-to-left ratio = 3:0) (**Fig. 8**) [19]. Our latest study also showed that the right-to-left ratios were 6:5 and 5:2 in SP and PC tumors, respectively, and CP tumors were dominantly supplied by RHA [27]. This tendency for the origin of the caudate artery in each subsegment is helpful in identifying the tumor feeder according to the tumor location.

In an analysis of 146 caudate HCCs (mean diameter, 2.6 cm; range, 0.5-4.0) by Yoon et al. [17], tumor feeders of SP were derived from RHA (55.5%), LHA (37.0%), and the proper or common hepatic artery (7.4%). In HCCs in PC, 90.2% of tumor feeders were derived from RHA, and the remaining feeders were derived from LHA and the proper or

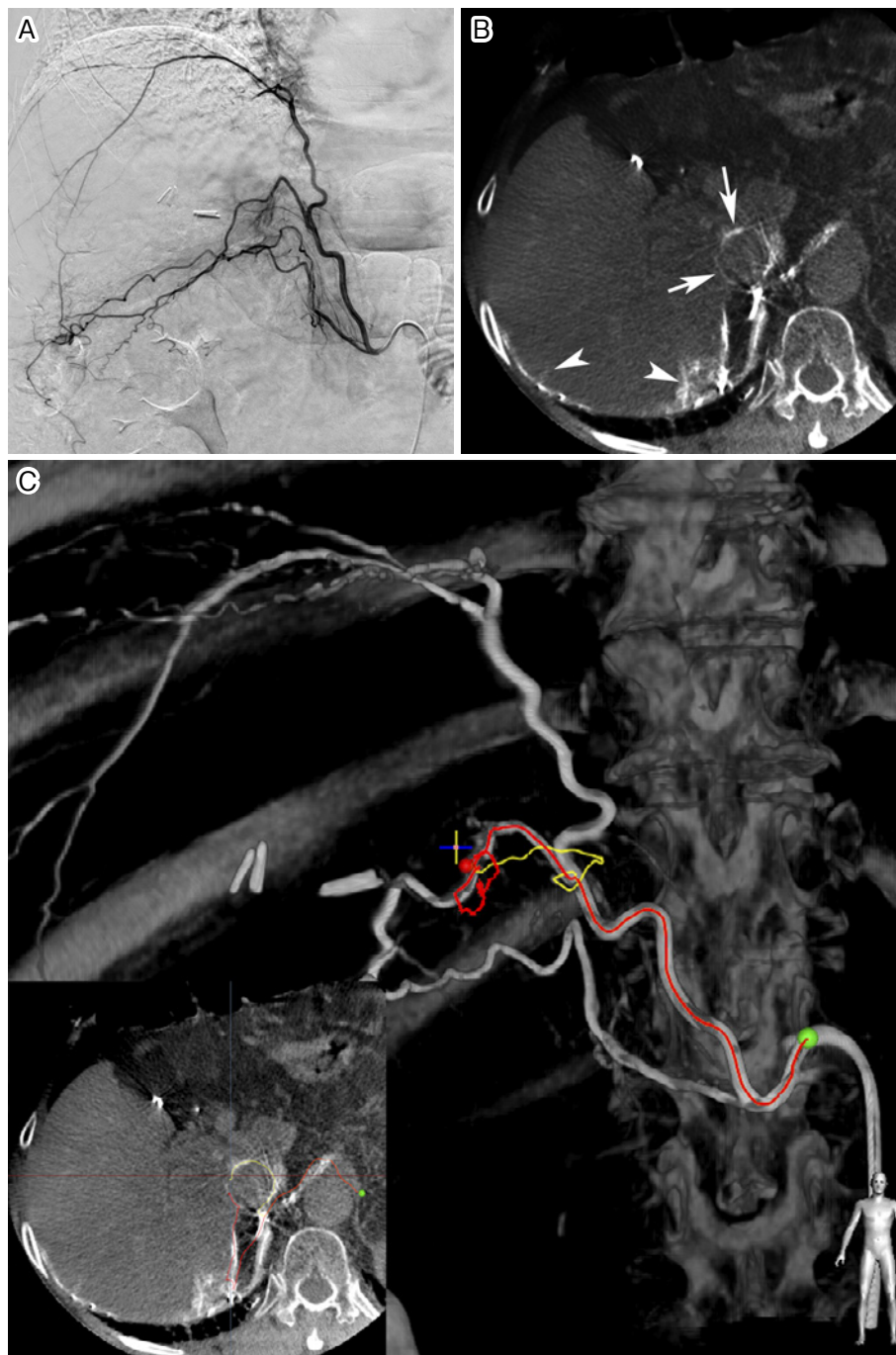


Figure 7. Blood supply to the caudate lobe from the right inferior phrenic artery (IPA). A. Arteriogram of the right IPA. B. Cone-beam CT during arteriography of the right IPA demonstrates that two branches run around the inferior vena cava (IVC) (arrows) and supplies the dorsal part of the Spiegel lobe. The branches of the posterior branch also enter the liver through the communication with the isolated arteries (arrowheads). C. Transarterial chemoembolization guidance software reveals that one branch arising at the bifurcation of the anterior and posterior branches (red) and another branch arising from the proximal portion of the posterior branch (yellow) penetrate the IVC ligament and run around the IVC.

common hepatic artery. In CP, all tumor feeders were derived from RHA. Their results in SP and CP tumors were almost equal to ours, but the results in PC tumors were quite different. This discrepancy might be caused by the different tumor size and ambiguous border of PC. Additionally, previous TACE through the neighboring branches of the caudate lobe might have changed the vascular territories of

the caudate arteries [18].

TACE for HCC in the Caudate Lobe

Because of the complex blood supply of the caudate lobe, 16%-31% of HCCs originating there are fed by multiple branches arising from different origins [17-20]. Additionally,

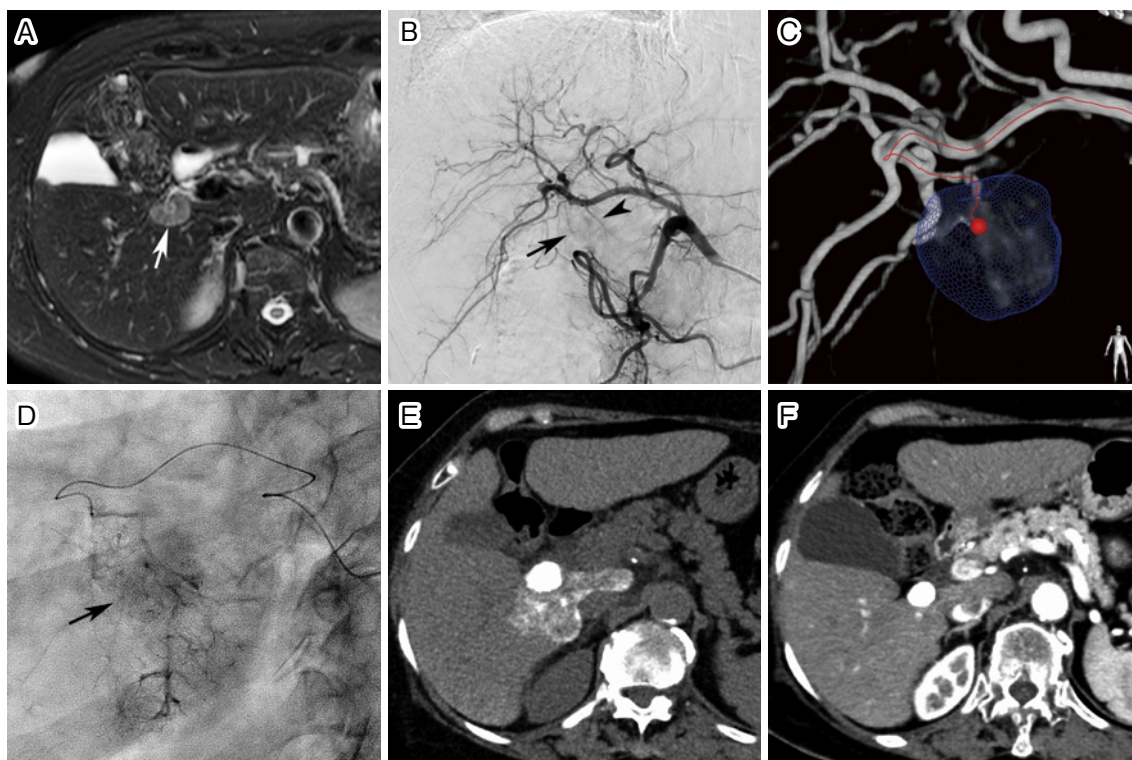


Figure 8. Usefulness of transarterial chemoembolization (TACE) guidance software for hepatocellular carcinoma in the caudate lobe.

A. T2-weighted MRI shows a tumor in the caudate process of the caudate lobe (arrow). B. Common hepatic arteriogram shows a tumor stain (arrow) and tumor-feeding branch (arrowhead), but the origin of the tumor feeder is unclear. C. TACE guidance software identifies the tumor feeder arising from the posterior segmental artery of the right hepatic artery. D. The branch was selectively embolized. The arrow indicates the tumor. E. Unenhanced CT performed 1 week after TACE shows dense iodized oil accumulation in the tumor. F. Arterial-phase CT performed 3 months after TACE shows no tumor recurrence.

the tumor-feeding branch of a recurrent tumor in the caudate lobe frequently changes on follow-up arteriograms because of the overlap of these vascular territories [17, 18, 24]. These factors might make it more difficult to control HCC in the caudate lobe with TACE [18-20].

With the advancement of microcatheter-guidewire technologies, the therapeutic effects of TACE for caudate lobe HCC have been improved. In a report by Kim et al. [38], the 5-year survival rate of patients with solitary HCC in the caudate lobe was 72% when the tumor-supplying caudate artery could be selectively embolized. Conversely, the 3-year survival rate reduced to 33% when selective catheterization into the caudate artery failed. Therefore, selective embolization of the caudate artery was a significant prognostic factor of overall survival ($P = 0.000$) and progression-free survival ($P = 0.013$) in patients with solitary HCC in the caudate lobe [38]. Nonselective TACE for HCC in the caudate lobe is ineffective because the caudate artery is small and usually arises from the proximal portion of the hepatic artery. Most embolic agents injected nonselectively flow away to the distal normal liver. Therefore, nonselective TACE is also associated with a risk of liver parenchymal injury.

The advancement of cone-beam CT (CBCT) technology has also improved the technical success of TACE [23, 27, 36, 39-48]. In a report by Choi et al. [23], more than 90%

of tumor-feeding arteries of caudate lobe HCCs could be identified by CBCT during hepatic arteriography (CBCTHA). Moreover, automated tumor feeder detection (AFD) software using CBCTHA data could identify 86% of tumor feeders of caudate lobe HCCs with a mean diameter of 18.6 ± 9.9 mm (range, 6-53 mm), and 75.9% of tumors could be completely embolized (Fig. 8) [27].

It is expected that CBCT and AFD can improve the technical success and therapeutic effect of TACE for HCC in the caudate lobe, but our latest analysis showed the different tumor feeder detection rates by AFD among three subsegments and no relationships between tumor feeder detectability and outcomes of TACE. The detection rate of tumor feeders was the highest (94.8%) in HCCs in PC, but the outcomes of TACE were reduced (technical success rate, 65.8%; and complete response [CR] rate, 59.4%). By contrast, feeder detectability was the lowest (71.4%) in HCCs in SP, but the outcomes of TACE were the best (technical success rate, 93.3%; and CR rate, 93.1%). In CP tumors, the rates of feeder detection, technical success of TACE, and CR were 76.5%, 63.6%, and 80.0%, respectively [27]. Our results suggest that PC is a watershed area between the bilateral hepatic lobes. Therefore, various branches can potentially feed the PC tumor. By contrast, feeders of HCCs in SP can also arise from various sites, but SP is "a peripheral

portion of the liver” and the branches that can enter SP are limited. As a result, favorable outcomes can be achieved when the tumor feeder is selectively embolized. CP tumors are likely to be supplied by small branches of RHA and/or its major branches [27], and arterial communications at the hepatic hilum can also promote collateral supply and can help tumor survival [16, 30-32].

Embolization Technique for HCC in the Caudate Lobe

A small microcatheter with a preshaped angled tip can facilitate selective catheterization into the caudate artery [48] because the caudate artery is small and usually arises from the large hepatic artery with an acute angle. Additional bending of the catheter tip by steam heat is frequently required when a microwire cannot be deeply advanced into it [18]. Preshaping of a microwire into the shepherd’s hook form (shepherd’s hook technique) and a steerable microcatheter or triaxial microcatheter system is also useful to directly select the sharply angled caudate artery [20, 49, 50].

When a microcatheter is advanced into the caudate artery, embolic materials should be injected slowly to avoid overflow. In particular, it should be carefully observed whether iodized oil accumulates in the main bile duct wall or flows into another branch through an anastomosis. Additionally, collateral blood flow through other caudate arteries may occasionally reverse the blood flow of the embolized artery and may prevent effective treatment (**Fig. 4**). In such a situation, the microcatheter should be advanced distal to the anastomosis [18]. In tumors fed by multiple feeders, embolizing the minor tumor feeder first can avoid pushing back of embolic materials by the reversed flow [48]. This technique also makes it possible to perform retrograde embolization of the main caudate artery through the anastomosis (Video 1). Moreover, branches that are opacified during iodized oil injection should be embolized, if possible (Video 2), because they may have the potential to feed the tumor after TACE [51].

When the catheterization of the caudate artery fails despite all efforts, the use of a microballoon catheter is recommended for distal protection [20]. Currently in Japan, a microballoon catheter with a side hole is commercially available and TACE under distal protection can be performed through one access route [52]. The usefulness of TACE under dual occlusion of the hepatic artery distal and proximal to the orifice of the unselectable caudate artery has also been reported [53]. To select the IPA that supplies the caudate HCC but cannot be selected by a conventional coaxial technique, a catheter with a large side hole or cleft (Video 2) or turn-back technique is useful [54-58]. If the tumor feeder arising from the extrahepatic artery cannot be selected, embolization with metallic coils distal to the orifice of the tumor feeder enables us to perform TACE safely [18, 20]. Coil embolization of the extrahepatic artery even supplying the alimentary tract is safe, but we should pay attention to the inadvertent occlusion of the tumor feeder by me-

tallic coils that are not correctly placed.

Conclusion

Although microcatheter-guidewire technologies and imaging modalities, including TACE guidance software, have been advanced, HCC in the caudate lobe is still difficult to completely embolize. Additionally, TACE of the caudate artery may cause bile duct necrosis. Therefore, we should recognize the peculiarity of the vascular anatomy of the caudate lobe and should be familiar with the techniques of selective catheterization and embolization of the caudate artery.

Conflict of Interest: The author has received lecture fees from Guerbet, Asahi Intecc, and Philips Healthcare.

Disclaimer: Shiro Miyayama is one of the Editorial Board members of Interventional Radiology. This author was not involved in the peer-review or decision-making process for this paper.

References

1. Tanaka S, Shimada M, Shirabe K, et al. Surgical outcome of patients with hepatocellular carcinoma originating in the caudate lobe. *Am J Surg*. 2005; 190: 451-455.
2. Shimada M, Matsumata T, Maeda T, Yanaga K, Taketomi A, Sugimachi K. Characteristics of hepatocellular carcinoma originating in the caudate lobe. *Hepatology*. 1994; 19: 911-915.
3. Shibata T, Maetani Y, Ametani F, Kubo T, Itoh K, Konishi J. Efficacy of nonsurgical treatments for hepatocellular carcinoma in the caudate lobe. *Cardiovasc Intervent Radiol*. 2002; 25: 186-192.
4. Seror O, Haddad D, N’Kontchou G, et al. Radiofrequency ablation for the treatment of liver tumors in the caudate lobe. *J Vasc Interv Radiol*. 2005; 16: 981-990.
5. Yamakado K, Nakatsuka A, Akeboshi M, Takaki H, Takeda K. Percutaneous radiofrequency ablation for the treatment of liver neoplasms in the caudate lobe left of the vena cava: electrode placement through the left lobe of the liver under CT-fluoroscopic guidance. *Cardiovasc Intervent Radiol*. 2005; 28: 638-640.
6. Terayama N, Miyayama S, Tatsu H, et al. Subsegmental transcatheter arterial embolization for hepatocellular carcinoma in the caudate lobe. *J Vasc Interv Radiol*. 1998; 9: 501-508.
7. Uchida H, Ohishi H, Matsuo N, et al. Transcatheter hepatic segmental arterial embolization using lipiodol mixed with an anticancer drug and Gelfoam particles for hepatocellular carcinoma. *Cardiovasc Intervent Radiol*. 1990; 13: 140-145.
8. Matsui O, Kadoya M, Yoshikawa J, et al. Small hepatocellular carcinoma: treatment with subsegmental transcatheter arterial embolization. *Radiology*. 1993; 188: 79-83.
9. Matsuo N, Uchida H, Nishimine K, et al. Segmental transcatheter hepatic artery chemoembolization with iodized oil for hepatocellular carcinoma: antitumor effect and influence on normal tissue. *J Vasc Interv Radiol*. 1993; 4: 543-549.
10. Miyayama S, Matsui O, Yamashiro M, et al. Ultrasensitive transcatheter arterial chemoembolization with a 2-F tip microcatheter for small hepatocellular carcinomas: relationship between local tumor recurrence and visualization of the portal vein with iodized oil. *J Vasc Interv Radiol*. 2007; 18: 365-376.
11. Miyayama S, Mitsui T, Zen Y, et al. Histopathological findings after ultrasensitive transcatheter arterial chemoembolization for hepatocellular carcinoma. *Hepatol Res*. 2009; 39: 374-381.

12. Miyayama S, Matsui O. Superselective conventional transarterial chemoembolization for hepatocellular carcinoma: rationale, technique, and outcome. *J Vasc Interv Radiol.* 2016; 27: 1269-1278.
13. Kumon M. Anatomy of the caudate lobe with special reference to portal vein and bile duct. *Acta Hepatol Jpn.* 1985; 26: 1193-1199. in Japanese.
14. Kogure K, Kuwano H, Fujimaki N, Makuuchi M. Relation among portal segmentation, proper hepatic vein, and external notch of the caudate lobe in the human liver. *Ann Surg.* 2000; 231: 223-228.
15. Kogure K, Kuwano H, Yorifuji H, et al. The caudate process hepatic vein: a boundary hepatic vein between the caudate lobe and the right liver. *Ann Surg.* 2008; 247: 288-293.
16. Oshiro Y, Sasaki R, Takeguchi T, Ibukuro K, Ohkohchi N. Analysis of the caudate artery with three-dimensional imaging. *J Hepatobiliary Pancreat Sci.* 2013; 20: 639-646.
17. Yoon CJ, Chung JW, Cho BH, et al. Hepatocellular carcinoma in the caudate lobe of the liver: angiographic analysis of tumor-feeding arteries according to subsegmental location. *J Vasc Interv Radiol.* 2008; 19: 1543-1550.
18. Miyayama S, Yamashiro M, Yoshie Y, et al. Hepatocellular carcinoma in the caudate lobe of the liver: variations of its feeding branches on arteriography. *Jpn J Radiol.* 2010; 28: 555-562.
19. Miyayama S, Yamashiro M, Hattori Y, et al. Angiographic evaluation of feeding arteries of hepatocellular carcinoma in the caudate lobe of the liver. *Cardiovasc Intervent Radiol.* 2011; 34: 1244-1253.
20. Kim HC, Miyayama S, Chung JW. Selective chemoembolization of caudate lobe hepatocellular carcinoma: anatomy and procedural techniques. *Radiographics.* 2019; 39: 289-302.
21. Miyayama S, Yamashiro M, Okuda M, et al. Main bile duct stricture occurring after transcatheter arterial chemoembolization for hepatocellular carcinoma. *Cardiovasc Intervent Radiol.* 2010; 33: 1168-1179.
22. Miyayama S, Yamashiro M, Hashimoto M, et al. Blood supply of the main bile duct from the caudate artery and medial subsegmental artery of the hepatic artery: Evaluation using images obtained during transcatheter arterial chemoembolization for hepatocellular carcinoma. *Hepatol Res.* 2013; 43: 1175-1181.
23. Choi WS, Kim HC, Hur S, et al. Role of C-arm CT in identifying caudate arteries supplying hepatocellular carcinoma. *J Vasc Interv Radiol.* 2014; 25: 1380-1388.
24. Miyayama S, Yamashiro M, Sugimori N, Ikeda R, Ishida T, Sakuragawa N. Blood supply to the caudate lobe of the liver from the right inferior phrenic artery: observation by cone-beam computed tomography during arteriography. *Abdom Radiol (NY).* 2020; 45: 2851-2861.
25. Miyayama S, Yamashiro M, Shibata Y, et al. Arterial blood supply to the caudate lobe of the liver from the proximal branches of the right inferior phrenic artery in patients with recurrent hepatocellular carcinoma after chemoembolization. *Jpn J Radiol.* 2012; 30: 45-52.
26. Woo S, Kim HC, Chung JW, et al. Chemoembolization of extrahepatic collateral arteries for treatment of hepatocellular carcinoma in the caudate lobe of the liver. *Cardiovasc Intervent Radiol.* 2015; 38: 389-396.
27. Miyayama S, Yamashiro M, Ikeda R, et al. Outcomes of conventional transarterial chemoembolization using guidance software for hepatocellular carcinoma in the caudate lobe of the liver. *Int J Gastrointest Interv.* 2023; 12: 75-82.
28. Stapleton GN, Hickman R, Terblanche J. Blood supply of the right and left hepatic ducts. *Br J Surg.* 1998; 85: 202-207.
29. Chen WJ, Ying DJ, Liu ZJ, He ZP. Analysis of the arterial supply of the extrahepatic bile ducts and its clinical significance. *Clin Anat.* 1999; 12: 245-249.
30. Vellar ID. The blood supply of the biliary ductal system and its relevance to vasculobiliary injury following cholecystectomy. *Aust N Z J Surg.* 1999; 69: 816-820.
31. Rath AM, Zhang J, Bourdelat D, Chevrel JP. Arterial vascularisation of the extrahepatic biliary tract. *Surg Radiol Anat.* 1993; 15: 105-111.
32. Tohma T, Cho A, Okazumi S, et al. Communicating arcade between the right and left hepatic arteries: evaluation with CT and angiography during temporary balloon occlusion of the right or left hepatic artery. *Radiology.* 2005; 237: 361-365.
33. Couinaud C. Surgical anatomy of the liver revisited. Paris, France: Couinaud; 1989. p.96-124.
34. Kobayashi K, Matsui O, Yoshikawa J, Kadoya M, Kawamori Y, Takashima T. Right hepatic arterial supply to the posterior aspect of segment IV of the liver: analysis by CT during hepatic arteriography. *Abdom Imaging.* 1999; 24: 591-593.
35. Miyayama S, Matsui O, Taki K, et al. Arterial blood supply to the posterior aspect of segment IV of the liver from the caudate branch: demonstration at CT after iodized oil injection. *Radiology.* 2005; 237: 1110-1114.
36. Miyayama S. Transarterial chemoembolization for hepatocellular carcinoma in the caudate lobe of the liver. *Kantansui.* 2021; 82: 727-737. in Japanese.
37. Miyayama S, Yamashiro M, Shibata Y, et al. Variations in feeding arteries of hepatocellular carcinoma located in the left hepatic lobe. *Jpn J Radiol.* 2012; 30: 471-479.
38. Kim HC, Chung JW, Jae HJ, et al. Caudate lobe hepatocellular carcinoma treated with selective chemoembolization. *Radiology.* 2010; 257: 278-287.
39. Miyayama S, Yamashiro M, Okuda M, et al. Usefulness of cone-beam computed tomography during ultraselective transcatheter arterial chemoembolization for small hepatocellular carcinomas that cannot be demonstrated on angiography. *Cardiovasc Intervent Radiol.* 2009; 32: 255-264.
40. Miyayama S, Yamashiro M, Hashimoto M, et al. Comparison of local control in transcatheter arterial chemoembolization of hepatocellular carcinoma ≤ 6 cm with or without intraprocedural monitoring of the embolized area using cone-beam computed tomography. *Cardiovasc Intervent Radiol.* 2014; 37: 388-395.
41. Deschamps F, Solomon SB, Thornton RH, et al. Computed analysis of three-dimensional cone-beam computed tomography angiography for determination of tumor-feeding vessels during chemoembolization of liver tumor: a pilot study. *Cardiovasc Intervent Radiol.* 2010; 33: 1235-1242.
42. Iwazawa J, Ohue S, Hashimoto N, Muramoto O, Mitani T. Clinical utility and limitations of tumor-feeder detection software for liver cancer embolization. *Eur J Radiol.* 2013; 82: 1665-1671.
43. Minami Y, Yagyu Y, Murakami T, Kudo M. Tracking navigation imaging of transcatheter arterial chemoembolization for hepatocellular carcinoma using three-dimensional cone-beam CT angiography. *Liver Cancer.* 2014; 3: 53-61.
44. Miyayama S, Yamashiro M, Hashimoto M, et al. Identification of small hepatocellular carcinoma and tumor-feeding branches with cone-beam CT guidance technology during transcatheter arterial chemoembolization. *J Vasc Interv Radiol.* 2013; 24: 501-508.
45. Miyayama S, Yamashiro M, Ikuno M, Okumura K, Yoshida M. Ultraselective transcatheter arterial chemoembolization for small hepatocellular carcinoma guided by automated tumor-feeders detection software: technical success and short-term tumor response. *Abdom Imaging.* 2014; 39: 645-656.
46. Miyayama S, Yamashiro M, Sugimori N, Ikeda R, Okimura K, Sakuragawa N. Outcomes of patients with hepatocellular carcinoma treated with conventional transarterial chemoembolization using guidance software. *J Vasc Interv Radiol.* 2019; 30: 10-18.

47. Iwazawa J, Ohue S, Hashimoto N, Muramoto M, Mitani T. Survival after C-arm CT-assisted chemoembolization of unresectable hepatocellular carcinoma. *Eur J Radiol.* 2012; 81: 3985-3992.
48. Miyayama S. Ultraselective conventional transarterial chemoembolization: When and how? *Clin Mol Hepatol.* 2019; 25: 344-353.
49. Soyama T, Yoshida D, Sakuhara Y, Morita R, Abo D, Kubo K. The steerable microcatheter: a new device for selective catheterization. *Cardiovasc Intervent Radiol.* 2017; 40: 947-952.
50. Shimohira M, Ogino H, Kawai T, Sakurai K, Nakagawa M, Shibamoto M. Clinical usefulness of the triaxial system in superselective transcatheter arterial chemoembolization for hepatocellular carcinoma. *Acta Radiol.* 2012; 53: 857-861.
51. Miyayama S, Matsui O. Transcatheter arterial chemoembolization using Lipiodol. In: Matsui O, Miyayama S, Osuga K, Ibukuro K, editors. *Transcatheter arterial chemoembolization (TACE) - Rationale and practical strategies.* Igaku-Shoin; 2015. p.140-168. in Japanese.
52. Yamagami T, Yoshimatsu R, Nishimori M, et al. Use of proximal side-hole micro-balloon catheter in transcatheter hepatic arterial chemoembolization. *Minim Invasive Ther Allied Technol.* 2017; 26: 372-376.
53. Soga S, Kuwamura H, Edo H, et al. Double balloon-occluded transarterial chemoembolization (double B-TACE) for hepatocellular carcinomas located in the caudate lobe. *Cardiovasc Intervent Radiol.* 2020; 43: 162-164.
54. Miyayama S, Matsui O, Akakura Y, et al. Use of a catheter with a large side hole for selective catheterization of the inferior phrenic artery. *J Vasc Interv Radiol.* 2001; 12: 497-499.
55. Miyayama S, Yamashiro M, Okuda M, et al. Creation of a cleft in an angiography catheter to facilitate catheterization of branches of the aorta arising at an acute angle. *J Vasc Interv Radiol.* 2008; 19: 1769-1771.
56. Miyayama S, Yamashiro M, Nagai K, Yokka A. Use of a catheter with a large side hole or cleft in selective catheterization of small branch arteries. *Intervent Radiol (Higashimatsuyama).* 2016; 1: 67-74.
57. Kim HC, Miyayama S, Choi JW, Kim GM, Chung JW. Hepatocellular carcinoma supplied by the inferior phrenic artery or cystic artery: anatomic and technical considerations. *Radiographics.* 2023; 43: e220076. doi: 10.1148/rg.220076.
58. Kiyosue H, Matsumoto S, Hori Y, Okahara M, Sagara Y, Mori H. Turn-back technique with use of a shaped microcatheter for superselective catheterization of arteries originating at acute angles. *J Vasc Interv Radiol.* 2004; 15: 641-643.

Interventional Radiology is an Open Access journal distributed under the Creative Commons Attribution-NonCommercial 4.0 International License. To view the details of this license, please visit (<https://creativecommons.org/licenses/by-nc/4.0/>).